PRAMANA
— journal of
physics

Vol. 66, No. 2
February 2006
pp. 403–414

Ionization and excitation of some atomic targets and metal oxides by electron impact

K N JOSHIPURA[1,*], B G VAISHNAV[2] and C G LIMBACHIYA[3]
[1]Department of Physics, Sardar Patel University, Vallabh Vidyanagar 388 120, India
[2]Sardar Vallabhbhai Patel Institute of Technology, Vasad 388 306, India
[3]P.S. Science College, Kadi 382 715, India
[*]E-mail: knjoshipura@yahoo.com

MS received 20 August 2005; revised 8 December 2005; accepted 29 December 2005

Abstract. We have calculated total inelastic and total ionization cross-sections for collisions of electrons on atomic targets oxygen (O), aluminium (Al) and copper (Cu) and metal oxides AlO and Al_2O, at impact energies from near excitation threshold to 2000 eV. A complex (optical) energy-dependent interaction potential is used to derive total inelastic cross-sections resulting from ionization as well as excitation processes. The inelastic cross-sections are bifurcated into discrete and continuum contributions and total ionization cross-sections have been deduced therefrom. Our calculation also provides information, hitherto sparse, on the excitation processes in the atomic targets O, Al, Cu and metal oxides AlO, Al_2O. Adequate comparisons are made with other theoretical and experimental data.

Keywords. Electron scattering; total cross-sections; atomic molecular ionization; complex potential.

PACS Nos 34.80.Bm; 34.80.Gs

1. Introduction

In this paper we have calculated total elastic as well as inelastic cross-sections of electron impact on O, Al, Cu atoms and metal oxides AlO and Al_2O. Electron collisional ionization of atomic and molecular targets poses a difficult theoretical problem involving three-body Coulomb interactions. It is necessary to pursue the problem even if approximately, in view of its importance in various applied fields. Total cross-sections for electron impact ionization and excitation of the atomic targets like oxygen are of great interest in aeronomy and astrophysical systems and in planetary atmospheres. The interpretation and modelling of spectral observations require the knowledge of collision cross-sections and radiative rate coefficients [1,2]. Collisions of electrons with atomic aluminium and copper together with their compounds (like AlO) find applications in different fields of research and industry, e.g. plasma physics and surface studies. Electrons impinging on solid targets

like aluminium and copper serve as important tools in electron microscopy, surface electron spectroscopy, micro-lithography and electron probe microanalysis [3]. The electron impact ionization studies of the metal oxide molecules of Al and Cu are important in materials research and are also found as impurities in the plasma edge of nuclear fusion reactors [4].

Various theoretical and experimental groups have so far examined electron scattering from the three atomic targets chosen presently. Total ionization cross-sections (TICS) in e–O scattering were measured by Thompson *et al* [5], while Johnson *et al* [2] performed experimental-cum-model studies on the VUV excitation–emission processes. The measured TICS of e–Al system have been due to Freund *et al* [6]. For e-Cu scattering, the TICS were measured by Freund *et al* [6], Bolorizadeh *et al* [7] and Bartlett and Stelbovics [8]. Two of the theoretical approaches currently in vogue for calculating electron–atom/molecule TICS are the binary encounter Bethe (BEB) theory of Kim and coworkers [9], and the Deusch-Maerk (DM) formulation [4]. The discrepancies found among the various earlier results call for yet another investigation on these atomic targets. For AlO and Al_2O molecules there is only one previous investigation [4]. Also, it is meaningful, as attempted presently, to assess the relative contribution of electron-induced discrete as well as continuum transitions in these atomic targets, within a common general formalism.

Thus, in the present work we have calculated basically the electron-induced total inelastic cross-sections $Q_{\rm inel}$, which are then bifurcated into the ionization and excitation contributions, at incident energies ranging from near threshold to 2000 eV. This is accomplished by starting with the well-known complex optical potential formalism. In recent years, we have developed and successfully employed a semi-empirical approach [10–14] called the 'complex scattering potential-ionization contribution' (CSP-ic) method to determine the total ionization cross-section $Q_{\rm ion}$ from the calculated $Q_{\rm inel}$, for a large number of atomic and molecular targets [10–14]. This method, highlighted below, is employed in the present calculations on O, Al and Cu, together with AlO and Al_2O.

2. Theoretical

At incident energies ($E_{\rm i}$) of the present interest, the inelastic channels in electron–atom scattering consist of discrete excitations and ionizations, and this enables us to express the total inelastic cross-section as,

$$Q_{\rm inel}(E_{\rm i}) = \sum Q_{\rm exc}(E_{\rm i}) + Q_{\rm ion}(E_{\rm i}). \tag{1}$$

In this break-up, the first term is the sum over total excitation cross-sections for all accessible transitions, while the second term indicates the total cross-section of all allowed ionization processes including auto-ionization of the target by the incident electrons. The first term arises mainly from the low-lying dipole allowed transitions for which the cross-sections become small progressively above the ionization threshold. Hence, as the incident energy increases the second term in eq. (1) dominates over the first, and this enables us to derive total ionization cross-section $Q_{\rm ion}$ if the inelastic quantity $Q_{\rm inel}$ is already calculated. This theoretical approach, to be called complex scattering potential-ionization contribution or CSP-ic method,

explores the advantages of the well-known complex-potential representation of simultaneous elastic and inelastic scattering, above the ionization threshold.

The present CSP-ic approach rests on spherical energy-dependent complex potential derived from the target electronic charge density $\rho(r)$, determined from accurate atomic wave functions [15]. The resulting total e–atom potential has a real part $V_{\rm R}$, which consists of static ($V_{\rm st}$), exchange ($V_{\rm ex}$) and polarization ($V_{\rm pol}$) terms. The imaginary potential term or the absorption potential $V_{\rm abs}$ is considered in the well-known quasi-free Pauli-blocking model of Staszeweska *et al* [16], after introducing some modifications discussed below. This is an energy-dependent potential that accounts for all possible inelastic scattering channels cumulatively, and has the generic form, in atomic units,

$$\begin{aligned} V_{\rm abs}(r, E_{\rm i}) &= -\frac{1}{2}\rho(r) v_{\rm loc}\sigma_{\rm ee} \\ &= -\rho(r)\left(\frac{T_{\rm loc}}{2}\right)^{1/2}\left(\frac{8\pi}{10k_{\rm F}^3 E_{\rm i}}\right) \\ &\quad \times\theta(p^2 - k_{\rm F}^2 - 2\Delta)(A_1 + A_2 + A_3). \end{aligned} \tag{2}$$

In the above expressions $v_{\rm loc}$ is the local speed of the external electron, and $\sigma_{\rm ee}$ denotes the average cross-section of the binary collision of the external electron with one of the target electrons.

The local kinetic energy of the incident electron is obtained from

$$T_{\rm loc} = E_{\rm i} - V_{\rm R} = E_{\rm i} - (V_{\rm st} + V_{\rm ex}). \tag{3}$$

In eq. (2), $p^2 = 2E_{\rm i}$, $k_{\rm F}$ is the Fermi wave vector and Δ is an energy parameter, that determines a threshold below which $V_{\rm abs} = 0$, and the ionization or excitation is prevented energetically. Further, $\theta(x)$ is the Heaviside unit step function, such that $\theta(x) = 1$ for $x > 0$, and is zero otherwise. The dynamic quantities A_1, A_2 and A_3 are specific functions of $\rho(r)$, I (ionization energy), Δ and $E_{\rm i}$. The role of Δ has been discussed in our recent publications. Briefly, if $\Delta = I$, then at an incident energy equal to or below I, not only ionization but excitation also will be prevented on account of $V_{\rm abs} = 0$. On the other hand, the excitation threshold $E_{\rm th}$ is rather small in many cases so that a choice $\Delta = E_{\rm th}$ would make $V_{\rm abs}$ excessively large. Hence the parameter Δ is taken to be a function of energy for $E_{\rm th} < E_{\rm i} \leq I$. For almost all the targets investigated by us [10–14] this choice of Δ results in a general accord of our calculations with the compared data. The next step is to solve the Schrödinger equation with the modified $V_{\rm abs}$, using the appropriate boundary conditions. Standard formulae [17] are used to generate $Q_{\rm inel}$ as well as $Q_{\rm el}$ by employing the complex phase shifts $\delta_l(k)$ for various angular momenta at different incident energies.

The inelastic cross-section $Q_{\rm inel}$ is not accessible directly in experiments, but in view of eq. (1), we have the relation,

$$Q_{\rm inel}(E_{\rm i}) \geq Q_{\rm ion}(E_{\rm i}). \tag{4}$$

At incident energies above I, the ionization begins to play a dominant role due to the availability of infinitely many open channels of scattering. There is no rigorous

way of projecting out $Q_{\rm ion}$ from the theoretical quantity $Q_{\rm inel}$. Perhaps a first ever estimate of ionization in relation to excitation processes was made by Turner *et al* [18]. They concluded from semi-empirical calculations that in gaseous water (H_2O), ionization was more probable than excitation above ∼30 eV. If $\sigma_{\rm ion}$ and $\sigma_{\rm exc}$ are the cross-sections of ionization and excitation respectively in their notation [18], then almost above 100 eV energy,

$$\frac{\sigma_{\rm ion}}{(\sigma_{\rm ion}+\sigma_{\rm exc})} \approx 0.75.$$

The usual complex potential calculations do not help us in determining ionization contribution separately, and hence further approximations are necessary. In the last few years we have introduced an approximation by defining a ratio,

$$R(E_{\rm i}) = \frac{Q_{\rm ion}(E_{\rm i})}{Q_{\rm inel}(E_{\rm i})}, \quad 0 \le R \lesssim 1. \tag{5}$$

Obviously $R = 0$ when $E_{\rm i} \le I$. For a number of stable atomic and molecular targets like Ne, Ar, O_2, CH_4, etc., for which the experimental cross-sections $Q_{\rm ion}$ are known accurately [19,20], the ratio R is found to rise steadily as the energy increases above the threshold (I), and approaching unity at high energies. Thus

$$R(E_{\rm i}) = 0, \quad \text{for } E_{\rm i} \le I, \tag{6a}$$
$$= R_{\rm p}, \quad \text{at } E_{\rm i} = E_{\rm p} \tag{6b}$$
$$\cong 1, \quad \text{for } E_{\rm i} > E_{\rm p}. \tag{6c}$$

Here, $E_{\rm p}$ stands for the incident energy at which our calculated cross-section $Q_{\rm inel}$ attains its maximum, while $R_{\rm p} \cong 0.7$ stands for the value of the ratio R at $E_{\rm i} = E_{\rm p}$. The choice of this value is approximate but physically justified. The peak position $E_{\rm p}$ (typically around 50 eV) occurs at an incident energy where the discrete excitation cross-sections are on the wane, while the ionization cross-section is rising fast, suggesting the $R_{\rm p}$ value to be above 0.5 but below 1. We follow the general observation [5–9,13] that at energies close to the peak of ionization, the contribution of the cross-section $Q_{\rm ion}$ is about 70–80% in the total inelastic cross-section $Q_{\rm inel}$ and it increases with energy. This behaviour is attributed to the faster fall of the first term $\sum Q_{\rm exc}$ in eq. (1). For targets like Al where auto-ionization becomes important at high energies, the value of $R_{\rm p}$ would be higher. The approximate value adopted for $R_{\rm p}$ introduces an uncertainty (0.75±0.05), i.e. roughly 10% at the average value (0.75).

Now, for determining $Q_{\rm ion}$ from $Q_{\rm inel}$ we need R as a continuous function of energy $E_{\rm i} \ge I$, and hence we represent [10–15] the ratio $R(E_{\rm i})$ in the following manner:

$$R(E_{\rm i}) = 1 - f(U),$$

i.e.,

$$R(E_{\rm i}) = 1 - C_1 \left[\frac{C_2}{U+a} + \frac{\ln(U)}{U}\right]. \tag{7}$$

Here U is the dimensionless variable defined through,

Table 1. Parameters for atomic targets O, Al and Cu.

Target atom	Ionization energy (eV)	Parameters					
		E_p (eV)	E_{ion} (eV)	a	C_1	C_2	R_p
O	13.62	70	100	6.925	−1.121	−7.073	0.70
Al	5.99	14	20	6.202	−1.620	−4.445	0.80
Cu	7.73	38	47	6.542	−1.704	−4.427	0.80

$$U = \frac{E_i}{I}, \quad U \geq I. \tag{8}$$

The reason for adopting a particular function for $f(U)$ in eq. (7) has also been discussed earlier [10–14]. As E_i increases above I, the ratio R increases and approaches the value 1, since the ionization contribution rises and the discrete excitation term in eq. (1) decreases. The discrete excitation cross-sections, dominated by dipole transitions, fall off as $\ln(U)/U$ at high energies. Accordingly the decrease of the function $f(U)$ must also be proportional to $\ln(U)/U$ in the high range of energy. However, the two term representation of $f(U)$ as above is more appropriate since the 1st term in the square bracket ensures a better energy dependence at low and intermediate E_i. Equation (7) involves dimensionless parameters C_1, C_2 and a, that reflect the target properties, since the three conditions stated in eqs (6a)–(6c) are used to determine these three parameters. To implement the third condition (6c) clearly, we first assume $a = 0$ and consider a two-parameter expression in eq. (7). Employing the two conditions (6a) and (6b) we first evaluate the C-parameters only. The resulting two-parameter expression is then used to obtain the value of R at a high energy $E_i = 10E_p$, and the same is employed in (6c). We have shown in table 1 the various parameters involved in the present work on O, Al and Cu along with C_1, C_2 and a evaluated as explained above. In atomic O there are several optically allowed channels below the first ionization threshold (13.6 eV) and hence $R_p = 0.7$ is reasonable.

Turning briefly to the present molecular targets AlO and Al_2O, let us mention that the present method has been applied successfully to a large number of molecules also. For the present molecular targets the charge density required as input is calculated as in [12–14]. The first ionization thresholds $I = 9.64$ eV for AlO and $I = 8.10$ eV for Al_2O have been employed appropriately in the present CSP-ic method.

3. Results, discussions and conclusions

We have employed in this paper, the semi-empirical approach (CSP-ic) which has been tested successfully earlier in predicting the TICS of a large variety of atomic and molecular targets. The theory outlined above offers the determination of the important cross-sections Q_{inel} and Q_{ion} along with a useful estimate on excitations in terms of $\sum Q_{exc}$. It is seen from the properties given in table 1 that the atoms

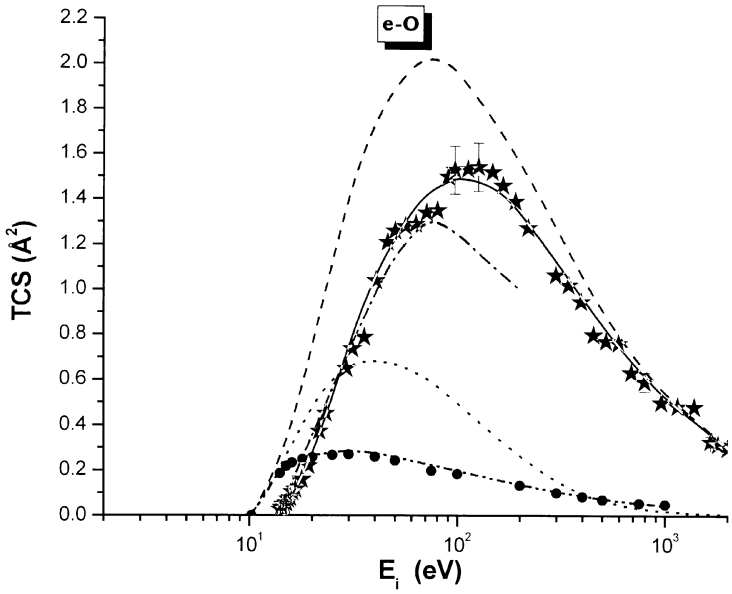

Figure 1. e–O Scattering. (- - -) present $Q_{\rm inel}$; (—) present $Q_{\rm ion}$; (. . .) present $\sum Q_{\rm exc}$; (- · -) DM [4] $Q_{\rm ion}$; experimental ($\star$) $Q_{\rm ion}$, Thompson *et al* [5]; ($\bullet$) $\sum Q_{\rm exc}$, Johnson *et al* [2]; (- ·· -) $\sum Q_{\rm exc}$, Johnson model [2].

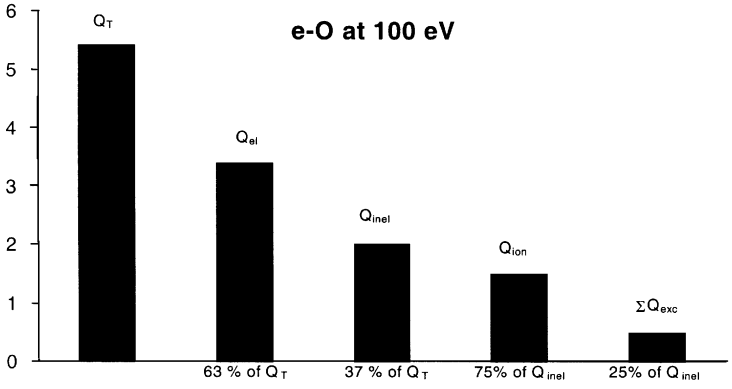

Figure 2. Various total cross-sections in (Å^2) of e–O scattering at 100 eV, showing the relative contribution at the ionization peak.

Al and Cu are more ionizable than atomic O. Accordingly the positions ($E_{\rm p}$) of the peak of the inelastic cross-section $Q_{\rm inel}$ in the two metallic atoms are expected to occur at a lower energy, and the peak magnitudes would be higher. That is indeed the case in figures 1 to 5 exhibiting the present theoretical results along with the compared data for oxygen, aluminium and copper atoms and the two metal oxides.

Although the e–O scattering has been investigated quite extensively by many workers so far, we present here in figure 1 and table 2 our cross-section results for

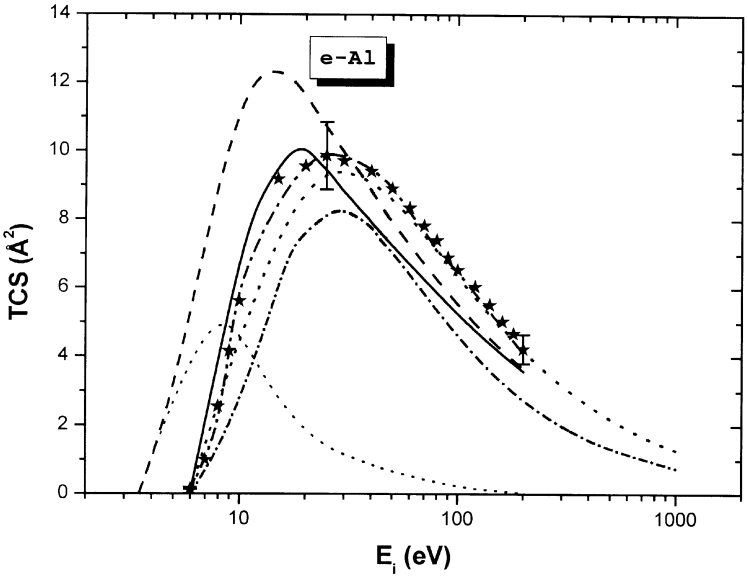

Figure 3. e–Al scattering. (– –) Present Q_{inel}; (—) present Q_{ion}; (- - -) BEB [9] Q_{ion}; (– · –) DM [4] Q_{ion}; (- · -) Bartlett [8] Q_{ion}; (. . .) present $\sum Q_{\text{exc}}$; experimental ($\star$) data, Freund *et al* [6].

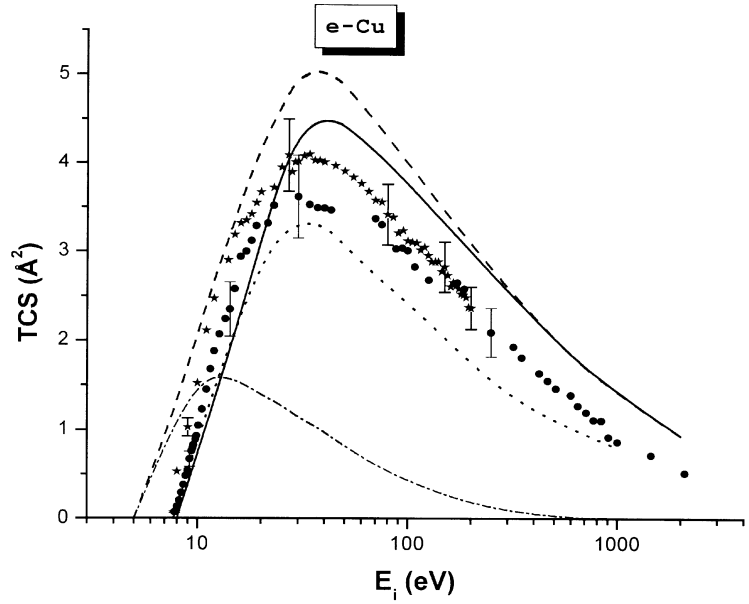

Figure 4. e–Cu scattering. (– –) Present Q_{inel}; (—) present Q_{ion}; (- - -) BEB [9] Q_{ion}; (- - -) Bartlett [8] Q_{ion}; (– · –) present $\sum Q_{\text{exc}}$; experimental ($\star$) Q_{ion} data of Freund *et al* [6]; (•) Bolorizadeh [7].

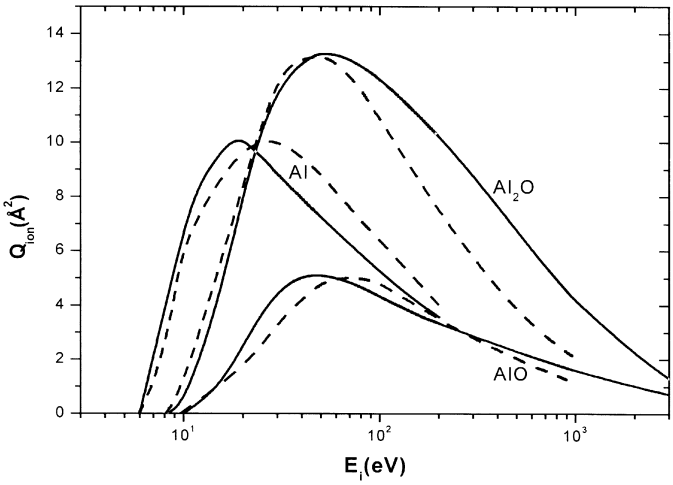

Figure 5. Al, AlO, Al_2O scattering: (—) present $Q_{\rm ion}$; (- -) DM [4] $Q_{\rm ion}$.

Table 2. Present total cross-sections ($Å^2$) of e–O scattering.

$E_{\rm i}$ (eV)	$\sum Q_{\rm ion}$	$\sum Q_{\rm exc}$	$Q_{\rm inel}$	$Q_{\rm el}$	$Q_{\rm T}$
20	0.26	0.49	0.75	6.54	7.29
30	0.75	0.66	1.41	5.66	7.07
50	1.22	0.67	1.89	4.68	6.57
80	1.45	0.57	2.02	3.85	5.87
100	1.51	0.50	2.01	3.40	5.41
200	1.35	0.26	1.61	2.24	3.85
300	1.13	0.15	1.28	1.72	3.00
500	0.84	0.064	0.904	1.05	1.95
700	0.67	0.035	0.705	0.72	1.43
1000	0.52	0.018	0.538	0.48	1.03
2000	0.30	0.004	0.304	0.16	0.46

a comparative study. There is no direct comparison for the cross-section $Q_{\rm inel}$ in any of the three atoms examined here. Our $Q_{\rm ion}$ values determined in the CSP-ic approach for O (figure 1) are in good accord with the experimental data of single plus double ionization of oxygen atoms, as measured by Thompson *et al* [5]. These measurements involve about 7% error at the peak. Thompson *et al* [5] had concluded that the effect of a possible admixture of metastable states of O should be small. The ionization calculations according to DM formalism [4], limited to 200 eV in all their investigations, are found to be on the lower side in this case. Our present calculations also seek to identify the relative importance of excitation as against ionization in the form of the summed-total excitation cross-sections $\sum Q_{\rm exc}$. Earlier results on discrete excitation processes reported prior to 1996, have been reviewed by Zecca *et al* [20]. We found a qualitative agreement, especially in the peak position, between the quoted results [20] on the sum of all excitation cross-sections

and the present $\sum Q_{\rm exc}$. We have not included these data [20] in figure 1, but let us note that near the peak position, i.e. at 45 eV, the earlier [20] data is higher than the present value. Johnson *et al* in USA [2] have investigated the electron-induced excitation–emission from atomic O in the VUV region. They have examined the four important transitions in O, viz., $2p^4\ {}^3P$-$3s^3S^0$ (130.4 nm), $2p^4\ {}^3P \rightarrow 3d^3D^0$ (102.7 nm), $2p^4\ {}^3P \rightarrow 3s'\ {}^3D^0$ (98.9 nm) and $2p^4\ {}^3P \rightarrow 3s''\ {}^3P^0$ (87.8 nm). We have included in figure 1, the sum total of their experimental total cross-sections (within 24% error) for these states. These authors [2] have also given model calculations (see figure 1) for the excitations of the said four states of O. The sum total of the excitation cross-sections of [2] provides a leading contribution to the quantity $\sum Q_{\rm exc}$ in our notation. The difference between the present excitation sum and the summed Johnson data [2] can be attributed partly to the low-lying states not included in [2], and partly to our own approximations. The said difference narrows down at energies beyond the ionization peak, as expected. At lower energies the present method is not reliable in view of the behaviour of the present absorption potential but still some important conclusions can be made. Thus, one finds from figure 1 that at about 25 eV the cumulative excitation and ionization cross-sections have an equal share in the $Q_{\rm inel}$. This observation supports a trend mentioned in [18] about the discrete versus continuum transitions in electron impact.

It is surprising but true that for the important e–O system there are no measurements of the total (complete) cross-sections $Q_{\rm T}$ or total elastic cross-sections $Q_{\rm el}$ above the ionization threshold, with the result that the sum-checks of various contributions like elastic scattering, excitation and ionization cannot be made. However, the present complex potential calculation on e–atom scattering yields the total cross-section $Q_{\rm T}$ through the following relation.

$$Q_{\rm T}(E_{\rm i}) = Q_{\rm el}(E_{\rm i}) + \sum Q_{\rm exc}(E_{\rm i}) + Q_{\rm ion}(E_{\rm i}).$$

In this context an interesting and useful study has been made presently in figure 2, where we show a bar chart for e–O collisions presenting the relative contribution of elastic scattering, ionization and the cumulative effect of excitations typically at 100 eV, i.e. near the ionization peak. Table 2 exhibits the important cross-sections of e–O scattering at various energies. At a high enough energy the $Q_{\rm T}$ of atomic oxygen is nearly half of the molecular oxygen value [19].

Turning now to e–Al scattering, our calculated results along with comparisons are exhibited in figure 3. From threshold to peak around 20 eV, the present $Q_{\rm ion}$ are in accord with the experimental data of Freund *et al* [6] involving 10% error. As mentioned by these experimentalists [6] the signals from double and higher ionization for Al were too weak to be measured. The DM formalism data [4] are in agreement with the present results. The BEB results shown in figure 3 are the total counting ionization cross-sections $Q_{\rm count}$ of the Al target calculated by Kim and Stone [9]. The cross-section $Q_{\rm count}$ [9] includes auto-ionization contribution as well as the small effect of multiple ionization cross-sections. In Kim and Stone [9] the direct ionization cross-section is calculated in their BEB model while the excitation–auto-ionization cross-section is estimated in a scaled plane-wave Born approximation only. These two cross-sections are added in [9] to obtain their final $Q_{\rm count}$ values, which we have plotted in figure 3 for comparison. While the present values and the DM results are closer to the measured data [6] from threshold to

the peak, the BEB values are in good accord with the measurements [6] beyond about 40 eV due to auto-ionization contribution from levels just above the ionization threshold. Now since the present complex potential calculation allows for all energetically accessible channels of inelastic scattering, the multiple ionization and auto-ionization are also included in our $Q_{\rm inel}$. The present $Q_{\rm inel}$ are relatively closer to the experimental data [6] above the $Q_{\rm ion}$ peak. The present results tend to agree with experiments [6] towards higher energies. In the case of electron impact excitation in Al there are no previous results. Hence the present indirect calculation of summed total excitation cross-section in Al shown by the lowest curve in figure 3 will provide a useful guideline.

The results on Cu atoms (figure 4) make an interesting study. In this case we have shown the latest measurements on $Q_{\rm ion}$ (single plus double ionization) available from the same paper of Freund *et al* [6]. Their measurements reported ionization signals even below the first ionization threshold (7.73 eV) of copper atoms in their ground state. This fact points to the presence of excited metastable Cu atoms in their atomic beam. The metastable species have a smaller ionization threshold and are responsible for the quick rise of the measured $Q_{\rm ion}$ from threshold to the peak, and also for the shift in the position of the peak to the left. It is for these reasons that our calculated $Q_{\rm ion}$ in figure 4 are lower than the data of Freund *et al* [6] for the rising part of the curve, and our peak position occurs at a slightly higher energy. The experimental data given by Bolorizadeh *et al* [7] are still lower, particularly up to about 100 eV. There are no DM or BEB calculations on Cu ionization, but we have included in this figure the single ionization calculations of Bartlett and Stelbovics [8] based on the Born approximation with full orthogonalization of the continuum Coulomb wave to all the occupied atomic orbitals. The Born results of [8] tend to agree with the present CSP-ic values at high enough energy, as one would expect. The lowest curve in figure 4 shows the excitation sum $\sum Q_{\rm exc}(E_{\rm i})$ for Cu atoms.

For the linear molecules of metal oxides AlO and Al_2O our calculated results along with comparisons including the Al atomic data are exhibited in figure 5. The DM formalism values [4] available are in a reasonably good agreement with the present results. The ordering of the maximum in the calculated ionization cross-sections for the Al-containing species is $Q_{\rm ion}({\rm AlO}) < Q_{\rm ion}({\rm Al}) < Q_{\rm ion}({\rm Al_2O})$, and this requires explanation. The maximum ionization cross-section of the AlO molecule is smaller than the maximum atomic Al ionization cross-section by almost a factor of 2, whereas the Al_2O cross-section exceeds the Al cross-section as well as the AlO cross-section, *vide* figure 5. The said ordering of Al, AlO and Al_2O cross-sections can be explained on the basis of atomic orbital populations and their contributions in the molecular structure [4]. This ordering as well as the peak position is understood in terms of the ionization thresholds, viz., $I({\rm AlO}) > I({\rm Al})$, along with the fact that Al_2O contains larger number of electrons.

In conclusion this paper presents our theoretical cross-sections of electron impact ionization and cumulative excitation processes in atomic and molecular targets (Al, Cu, O, AlO and Al_2O) at energies ∼5–2000 eV. The non-rigorous nature of the present approach prevents us from making a definitive prediction of the cross-sections but we have made sufficient comparisons here in order to arrive at certain conclusions. The present ionization results are generally on the higher side

but reliable within about 10–15% margin. The summed excitation cross-sections deduced presently are less certain but they serve to indicate an upper bound of the sum of individual experimental or theoretical excitation cross-sections for a target. Our discussion in §3 hints at the presence of metastable species in the experimental data on Cu [6]. It is clear from the example of the Al–AlO–Al_2O sequence that the present CSP-ic method correctly reproduces the dependence of the peak position and magnitude of TICS on the respective ionization threshold and the number of target electrons. Finally it is useful to have a theoretical picture showing the relative importance of different electron-collision processes at typical impact energy, as exhibited in the bar chart of various total cross-sections of the e–O system (figure 2). The corresponding cross-section values are given at selected energies in table 2. Theoretical results on CuO ionization by electron impact are not shown here but are available with the authors.

Acknowledgement

KNJ thanks the Indian Space Research Organization (Bangalore, India) for a research grant under which a part of this work was done.

References

[1] I Kanik, P V Johnson, M B Das, M A Khakoo and S S Tayal, *J. Phys. At. Mol. Opt. Phys.* **B34**, 2647 (2001)
[2] P V Johnson, I Kanik, D E Shemansky and X Liu, *J. Phys. At. Mol. Opt. Phys.* **B36**, 3203 (2003)
[3] Z Chaoui and N Bouarissa, *Phys. Lett.* **A297**, 432 (2002)
[4] H Deutsch, K Hilpert, K Becker, M Probst and T D Märk, *J. Appl. Phys.* **89**, 1915 (2001)
[5] W R Thompson, M B Shah and H B Gilbody, *J. Phys. At. Mol. Opt. Phys.* **B28**, 1321 (1995)
[6] R S Freund, R C Wetzel, R J Shul and T R Hayes, *Phys. Rev.* **A41**, 3575 (1990)
[7] M A Bolorizadeh, C J Patton, M B Shah and H B Gilbody, *J. Phys. At. Mol. Opt. Phys.* **B27**, 175 (1994)
[8] P L Bartlett and A T Stelbovics, *Phys. Rev.* **A66**, 012707 (2002)
[9] Y K Kim and P M Stone, *Phys. Rev.* **A64**, 052707 (2001)
[10] K N Joshipura, V Minaxi and U M Patel, *J. Phys. At. Mol. Opt. Phys.* **B34**, 509 (2001)
[11] K N Joshipura and C G Limbachiya, *Int. J. Mass Spectrom.* **216**, 239 (2002)
[12] K N Joshipura, B K Antony and V Minaxi, *J. Phys. At. Mol. Opt. Phys.* **B35**, 4211 (2002)
[13] K N Joshipura, M Vinodkumar, B K Antony and N J Mason, *Eur. Phys. J.* **D23**, 81 (2003)
[14] K N Joshipura, B K Antony, V Minaxi and C G Limbachiya, *Phys. Rev.* **A69**, 022705 (2004)
[15] C F Bunge, J A Barrintos and A V Bunge, *At. Data Nucl. Data* **53**, 113 (1993)
[16] D Staszewska, D W Schwenke, D Thirumalai and D G Truhlar, *Phys. Rev.* **A29**, 3078 (1984)

[17] C J Joachain, *Quantum collision theory* (North Holland Press, 1983) p. 110
[18] J E Turner, H G Paretzke, R N Hamm, H A Wright and R H Richie, *Radiat. Res.* **92**, 47 (1982)
[19] G P Karwasz, R S Brusa and A Zecca, *La Rivista Del Nuovo Cimento* **24**, 1 (2001)
[20] A Zecca, G P Karwasz and R S Brusa, *La Rivista Del Nuovo Cimento* **19**, 1 (1996)